fishes

MDPI

Article

Age, Growth and Population Structure Analyses of the *Berryteuthis magister shevtsovi* in the Japan Sea by Statolith Microstructure

Huajie Lu [1,2,3,4,*], Yuzhe Ou [1], Yurong Teng [1], Ziyue Chen [1] and Xinjun Chen [1,2,3,4]

[1] College of Marine Sciences, Shanghai Ocean University, Shanghai 201306, China
[2] Key Laboratory of Marine Ecological Monitoring and Restoration Technologies, MNRs, Shanghai 201306, China
[3] National Distant-Water Fisheries Engineering Research Center, Shanghai Ocean University, Shanghai 201306, China
[4] Key Laboratory of Oceanic Fisheries Exploration, Ministry of Agriculture, Shanghai Ocean University, Shanghai 201306, China
* Correspondence: hjlu@shou.edu.cn; Tel.: +86-021-61900318

Abstract: *Berryteuthis magister shevtsovi* is a new subspecies in the Japan Sea, and thus, little is known about its fisheries biology, especially age and population structure. Based on the 296 samples collected by the Chinese commercial jigging vessel in December 2018 in the Japan Sea. The age, growth, and population structure of *B. magister shevtsovi* were studied based on the microstructure of the statolith. The results indicated that the range of mantle length (ML) was 90–148 mm for females and 94–141 mm for males, the body weight (BW) ranged from 49 to 116 g and 38 to 110 g for females and males, and the ages were estimated from 52 to 166 days for females and 51 to 143 days for males, respectively. The hatching date extended from March to October, with a peak from July to September, suggesting the presence of one spawning group (summer–autumn group). The ANCOVA showed that there was no significant sex difference between the ML and BW growth; however, there was a significant difference between the sexes in the relationship between ML–age and BW–age. The relationship between the ML and BW was best described by the power function, the ML–age relationship of females was best described by linear function; the ML–age relationship of males and BW–age relationships of females and males were best described by the exponential function. *B. magister shevtsovi* is a high-growing squid, and the growth rate seemed to be high at the young life stage and decreased after the subadult stage (60–120 days older). This study provided basic information on the age, growth, and population structure of *B. magister shevtsovi*.

Keywords: *Berryteuthis magister shevtsovi*; statolith; age; growth pattern; Japan Sea

Citation: Lu, H.; Ou, Y.; Teng, Y.; Chen, Z.; Chen, X. Age, Growth and Population Structure Analyses of the *Berryteuthis magister shevtsovi* in the Japan Sea by Statolith Microstructure. *Fishes* **2022**, *7*, 215. https://doi.org/10.3390/fishes7050215

Academic Editor: Gioele Capillo

Received: 29 July 2022
Accepted: 22 August 2022
Published: 24 August 2022

1. Introduction

Berryteuthis magister shevtsovi is a cold-water oceanic pelagic cephalopod species with a wide distribution in the sea area of 35°00′ N–39°00′ N, 130°35′ E–134°00′ E and a distribution in the water layer of 200–600 m [1]. *B. magister shevtsovi* is a new subspecies [2] and has certain development potential. Some studies have been carried out on the existence of three subspecies of *B. magister shevtsovi*, which are abundant and geographically widespread in the North Pacific, including Japan, Okhotsk, the Bering Sea, and the Gulf of Alaska [2,3]. The annual life cycle of *B. magister shevtsovi* is approximately 1 year, similar to most oceanic cephalopods [4]. The subspecies in the Japan Sea is small, with a large fin, a bicuspid lateral tooth on radula, and weak differentiation between the central and marginal suckers on the tentacular club [1]. In recent years, little research has been done on the fisheries biology of the *B. magister shevtsovi*; only Wang Honghao [2], Chen Xuanyu [5], and Zhu Wenbin [6] have done research on basic biology.

The statolith structure exhibits a certain synchronization with the growth of the squid and can store rich life history information [7,8], which is characterized by a stable

structure, corrosion resistance, and irreversible deposition [9]. Population genetic exchange and harsh environmental conditions can lead to changes in the morphology of statolith microstructures, so it is one of the important carriers for studying the life history of cephalopods [10,11]. Therefore, squid statoliths are often used as a tool for studying age and growth, population structure, and life history [2,12]. Consistent with the growth patterns of beak, statolith growth can be measured as one daily concentric increment representing one day at the larval stage; this makes it easy to determine the ages of squid [12,13]. In general, previous age and growth studies were mostly analyzed through statoliths for cephalopods, and the early age and growth pattern studies on squids were mainly analyzed by periodic deposition increments of statolith microstructure [14]. At present, there are a few studies on statoliths of the *B. magister shevtsovi*, and there are no studies on the age and population structure based on the *B. magister shevtsovi* statolith.

B. magister shevtsovi is one of the new subspecies in the Japan Sea, and little is known about its fisheries biology, especially age and population structure. The purpose of this study is to provide basic information on the age, growth, and population structure of *B. magister shevtsov* in this water based on statolith microstructure analysis according to the data collected by the jigging vessel of *Zhouyu 678* in December 2018 to help in the assessment and management of this important species.

2. Materials and Methods

2.1. Sampling

A total of 296 samples of *B. magister shevtsovi* were collected by the Chinese commercial jigging vessel *Zhouyu 678* in December 2018 in the 35°00′ N–39°00′ N, 130°35′ E–134°00′ E area in the Japan Sea. About 15–20 samples were collected randomly once based on the different investigate locations and times. The samples were frozen on board immediately and brought back to the laboratory for further research. During the experiment, there were 34 statolith ages of *B. magister shevtsovi* were not obtained. The remaining 261 *B. magister shevtsovi* samples were analyzed in this paper, including 150 female samples and 111 male samples.

2.2. Basic Biological Determination and Statolith Extraction

The fishery biological data were measured after thawing the samples, and the mantle length (ML) and body weight (BW) were measured to accuracies of 1 mm and 1 g, respectively, and the sex and maturity stage were identified through visual examinations [15]. The female reproductive organs are mainly composed of nidamental gland, oviducal glands, and accessory glands. The male reproductive organs are mainly composed of spermatophoric gland, spermatophores, and accessory glands [16]. According to the original standard gonadal morphological characteristics, the samples of different sexes were divided into five maturity stages (immature: I and II; maturing: III; and mature: IV and V) [17,18]. In this experiment, 296 pairs of complete statolith samples from *B. magister shevtsovi* were extracted, washed, and stored in a centrifugal tube with 75% ethanol for age determination [19].

2.3. Statolith Processing and Aging

The improved statolith aging methodology was used in this study [20]. It is assumed that statoliths grow in one ring every day [21], and the number of daily rings was read to obtain the daily age data of statoliths of *B. magister shevtsovi* in this study. We chose the statoliths, as this region exhibits many dark, periodic longitudinal bands that can be easily used to interpret the age of the squid. After cleaning with water, the statoliths were placed flat in a plastic mold and hardened in a plastic mold with gradually caking epoxy [22]. The focal plane sample was ground on a sander with coarse sandpapers of different sizes (grit: 120, 600, 1200, and 2000) and then polished with an alumina solution on smooth sandpaper (2400) to remove scratches until the age cycle increments were clearly visible on the surface of the sample.

Different parts of the statoliths were observed using an Olympus microscope and photographed by a charge-coupled device (CCD) at different magnifications (×10, ×20,

×40, ×100, ×200, ×400). Then, an intact picture was consolidated using Photoshop CS 24.0 for the subsequent age estimation. Statolith microstructure was used to estimate cephalopod incremental readings with high accuracy and low coefficient of variation (CV% < 5%), indicating that the counting method was reliable [23]. To reduce bias in the age estimation process, the age information of a sample was considered to reflect the effective squid age when the difference between the average ages identified by two readers (each reader reads one statolith three times) was less than 10% [17]. Based on the statolith daily increments, we decided to back-calculate the hatching date and explore the growth patterns of the *B. magister shevtsovi* specimens living in the Japan Sea.

2.4. Data Analysis

Based on the obtained biological data, the following models were used to quantify the relationships between ML–BW, ML–age, and BW–age. Analysis of covariance (ANCOVA) was used to evaluate whether differences existed in the ML–BW, ML–age, and BW–age growth patterns between females and males.

Linear function [24]:

$$L_t = a + b\,t \tag{1}$$

Exponential function [25]:

$$L_t = a\,e^{\,b\,t} \tag{2}$$

Power function [26]:

$$L_t = a\,t^{\,b} \tag{3}$$

Logarithmic function [27]:

$$L_t = a\,ln(t) + b \tag{4}$$

where L_t is the ML (in mm)/BW (in g) at age t; t is the squid age (in days); and a and b are the parameters to be estimated.

For the above four models, the Akaike information criterion (*AIC*) of each model was calculated using the following equation [28,29].

$$L(data/\theta) = \prod_{i=1}^{n} \frac{1}{\delta\sqrt{2\pi}} \exp\left[-\frac{(y - f(t))^2}{2\delta^2}\right] \tag{5}$$

$$AIC = -r\,2\,ln\,(L_{max}) + 2\,m \tag{6}$$

where $L(data/\theta)$ is the likelihood of observing the data given parameters θ; vector θ denotes parameters to be estimated; y and $f(t)$ are the observed values for the featured parameters and the estimated values from the model, respectively; n is the number of observations; m is the number of model parameters; and L_{max} is the maximum value of $L(data/\theta)$ [28,30]. Competing models were compared by the Akaike weight (AIC_w) [29,31] computed as:

$$AIC_w\left(M_j \times \{M_j\}\right) = \frac{e^{-1/2(AIC_j - AIC_{min})}}{\sum_j^j e^{-1/2(AIC_j - AIC_{min})}} \tag{7}$$

where M_j is the series of j competing models and AIC_{min} is the lowest value among competing models. The Akaike weight (AIC_w) ranges between 0 and 1, with 1 indicating the best possible fit [31].

The absolute daily growth rates (AGRs, in mm/d or g/d) and instantaneous growth rates (IGRs, in %/d) of the ML and BW were estimated at each 20-day interval. The IGRs and AGRs were calculated using the following functions [19]:

$$AGR = (R_2 - R_1)/(t_2 - t_1) \tag{8}$$

$$IGR = [ln(R_2) - ln(R_1)]/(t_2 - t_1) \tag{9}$$

where R_1 and R_2 are the ML or BW means at the start (t_1) and end (t_2) of the time interval, respectively.

All statistical analyses were conducted in R (v.4.0.3 Foundation for Statistical Computing, Vienna, Austria) and Excel (2019, Microsoft office, USA).

3. Results

3.1. Individual Composition and Shape Features

The mantle of the *B. magister shevtsovi* was conical, with smaller body size and larger fins. Anterior and posterior fin edges straight; anterior lobes of fin distinct; lateral margins slightly rounded. The fin length was about 1/2 of the ML (Figure 1).

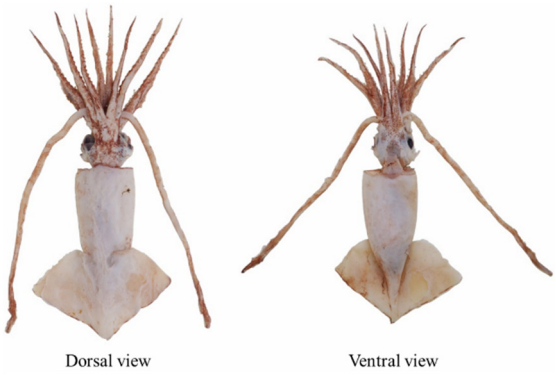

Figure 1. Appearance of *B. magister shevtsovi*.

The ANCOVA results showed that there were significant differences in the ML (F = 14.622, $p < 0.05$) and BW (F = 24.282, $p < 0.05$) between the sexes; thus, the ML and BW composition in *B. magister shevtsovi* could be divided into males and females. For all samples, the ML and BW ranged from 90–148 mm and 38–116 g, respectively. Therefore, with group interval of 10 mm and 20 g, the samples were divided into six ML groups and five BW groups, respectively.

The range of ML was 90–148 mm with an average of 112.06 mm and a high concentration in 110–130 mm, accounting for approximately 74.70 percent for females, and 94–141 mm with an average of 116.88 mm and a high concentration in 101–120 mm, accounting for 70 percent for males (Figure 2a).

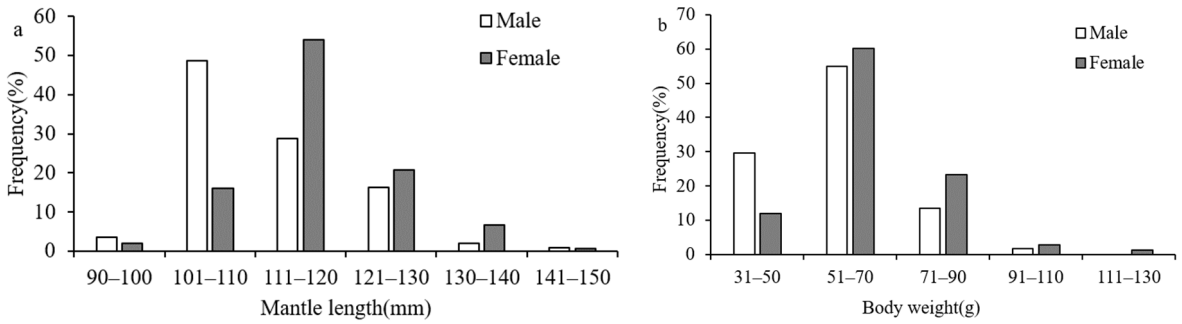

Figure 2. Distribution of ML (**a**) and BW (**b**) of *B. magister shevtsovi*.

The range of BW was 49–116 g with an average of 58.48 g and a high concentration of 50–90 g, accounting for 68.5 percent for females, and 38–110 g with an average of 61.12 g and a high concentration of 50–70 g, accounting for 84.70 percent for males (Figure 2b).

3.2. Microstructures of the Statolith

The growth rings of the statolith of *B. magister shevtsovi* were composed of alternating light and dark rings. According to the changes in the brightness and width of growth rings, the statoliths were divided into three main growth zones found in the dorsal dome of *B. magister*

shevtsovi from the nuclear (Figure 3a) toward the edge of the dorsal dome: the postnuclear zone (P, Figure 3b), dark zone (DZ, Figure 3c,d), and peripheral zone (PZ, Figure 3e) for all individuals were examined. Figure 3f was not in the reading direction of growth rings and was not used for counting to ensure the integrity of the statolith microstructure.

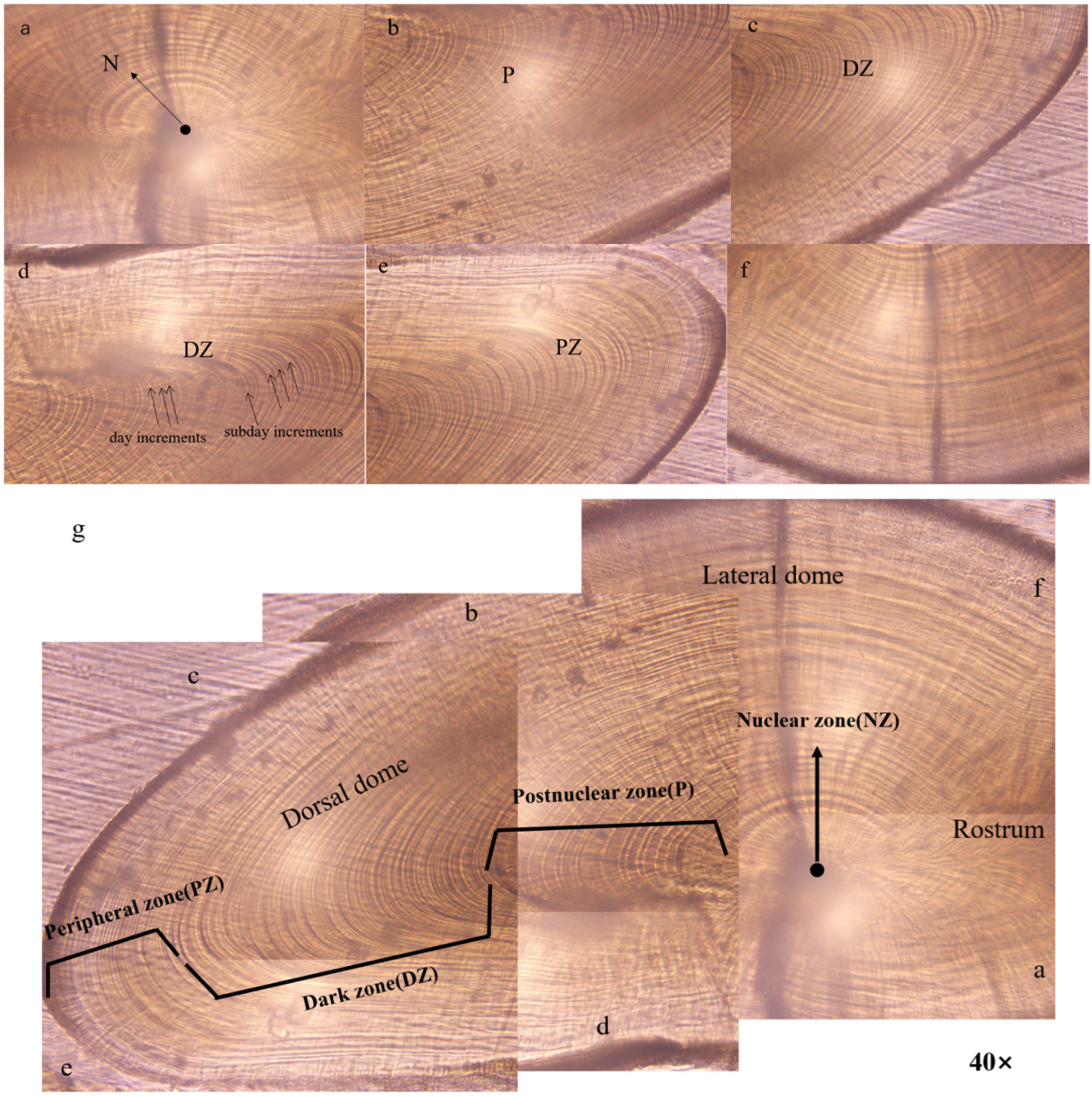

Figure 3. Statolith microstructure of *B. magister shevtsovi* (female with mantle length 110 mm, body weight 63 g, age 138 d). (**a**) showing the nuclear zone (N) within the zero ring; (**b**) showing the postnuclear zone (P); (**c**,**d**) showing the dark zone (DZ), and (**d**) showing the day increments and subday increments; (**e**) showing the peripheral zone (PZ); (**f**) ensure the integrity of the statolith microstructure; (**g**) showing three distinct growth zones with different incremental width.

Growth increments in the DZ were significantly wider than those in the P and PZ. The focus was the starting point of statolith growth and was slightly darker (Figure 3g). The NZ was the zone within the zero ring, which was usually in the shape of a droplet and darker in color (Figure 3a). The lateral dome of the statolith, namely, P and DZ, was relatively dark in color, and subday increments were found in DZ (Figure 3d). The growth rings in these zones were clearly visible, the width and spacing of the rings were relatively uniform, and

their growth rings were easy to read. The dorsal dome, that is, PZ, has uniform growth rings that are easy to read. Overall, from the NZ to the lateral dome, the brightness changes from dark to bright and then to dark, and the width of the growth rings changes from narrow to wide. From the lateral dome to the outer edge of the dorsal dome, the brightness was also from dark to bright and then to dark, but the width of the growth rings was from wide to narrow. Among them, PZ had the narrowest growth rings, followed by P, and DZ had the widest rings. There was no obvious boundary between these three zones, which cannot be clearly distinguished (Figure 3g).

3.3. Age Structure and Maturity

Results of this study, a total of 261 statolith ages were obtained, including 150 females and 111 males. The total sample ages ranged from 41–166 days (mean age 95.93 ± 20.329), with the majority (86.59%) of samples being from 60–120 days (Figure 4).

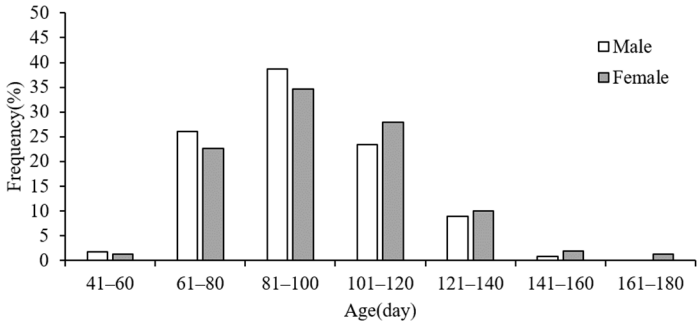

Figure 4. Age frequency distribution of *B. magister shevtsovi* by sex.

The age ranged from 52 to 142 days with an average of 93.39 days and a high concentration from 60–120 days, accounting for 88.29 percent for females (Figure 4). The ages ranged from 51 to 166 days with an average of 95.93 days and a high concentration from 60–140 days, accounting for 85.33 percent for males (Figure 4).

The youngest *B. magister shevtsovi* sample was male, with age of 51 days, the ML was 94 mm, the BW was 49 g, and the sexual maturity was stage II. The oldest *B. magister shevtsovi* sample was female, with an age of 166 days, the ML was 148 mm, the BW was 110 g, and the sexual maturity was stage IV.

The results of this study showed that most of the male and female sexual maturity of the *B. magister shevtsovi* were in stages I and II, the number of samples in stages III and IV was small, and no individuals in stage V were found. Among them, the proportion of female samples with stages I–IV sexual maturity was 52.67%, 32.00%, 12.00%, and 3.33%, respectively. The proportion of male samples with stage I–IV sexual maturity was 45.05%, 32.53%, 15.32%, and 7.20%, respectively (Figure 5).

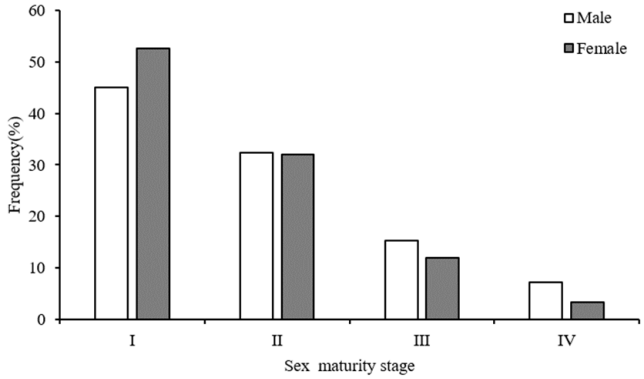

Figure 5. Maturity stage compositions of the *B. magister shevtsovi* by sex.

3.4. Hatching Date and Group

All of the samples in this study hatched from March to October 2018, suggesting that *B. magister shevtsovi* likely spawned throughout the year. The hatching dates of the squid samples were estimated by combining the age data and catching date information. The hatching dates of the *B. magister shevtsovi* samples collected in 2018 ranged from March to October, with the majority (80.5%) being distributed from August to September (Figure 6).

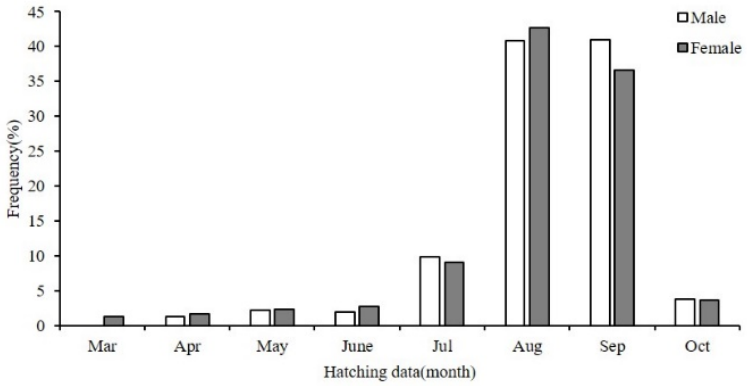

Figure 6. Hatching date frequency distribution of *B. magister shevtsovi* by sex.

The results showed that the hatching date of female squid was from March to October 2018. Male hatching dates were from April to October 2018. The peak period of female and male hatching was from August to September 2018, accounting for 79.24% and 81.76%, respectively (Figure 6). This demonstrated one dominant autumn group for *B. magister shevtsovi* squid.

3.5. Growth Pattern

The ANCOVA results showed that there were no significant differences between the sexes in the relationship between ML and BW of *B. magister shevtsovi* ($F = 0.442$, $p = 0.592 > 0.05$), but there were significant differences between the sexes in the relationship between ML–age ($F = 18.787$, $p = 0.000 < 0.05$) and BW–age ($F = 10.243$, $p = 0.002 < 0.05$).

Based on the lowest derived AIC value (Table 1), the BW–ML relationship was best described by the power growth model (Figure 7a), the ML–age relationship of females was best described by linear growth model (Figure 7b), the ML–age of males and BW–age relationships of females and males were best described by the exponential growth models (Figure 7b,c).

Table 1. Parameters of the linear, power, exponential, and logarithmic growth models fitted to the BW–ML, ML–age and BW–age relationships of the *B. magister shevtsovi* samples.

Year	Growth Model	Linear		Power		Exponential		Logarithmic	
		R^2	*AIC*	R^2	*AIC*	R^2	*AIC*	R^2	*AIC*
Females	ML–BW	0.7362	1077.0901	0.7420	861.2017	0.7388	861.2090	0.7259	861.2140
	ML–age	0.5939	1268.3508	0.5914	1306.3009	0.5918	1270.1061	0.5848	1452.1809
	BW–age	0.5686	1202.2370	0.558	1251.1959	0.6088	1200.7663	0.5128	1203.5403
Males	ML–age	0.6125	1273.8008	0.5925	1278.9351	0.6214	1269.5682	0.5761	1270.8557
	BW–age	0.6025	1299.3064	0.6030	1349.9067	0.6397	1299.0834	0.5540	1300.8069

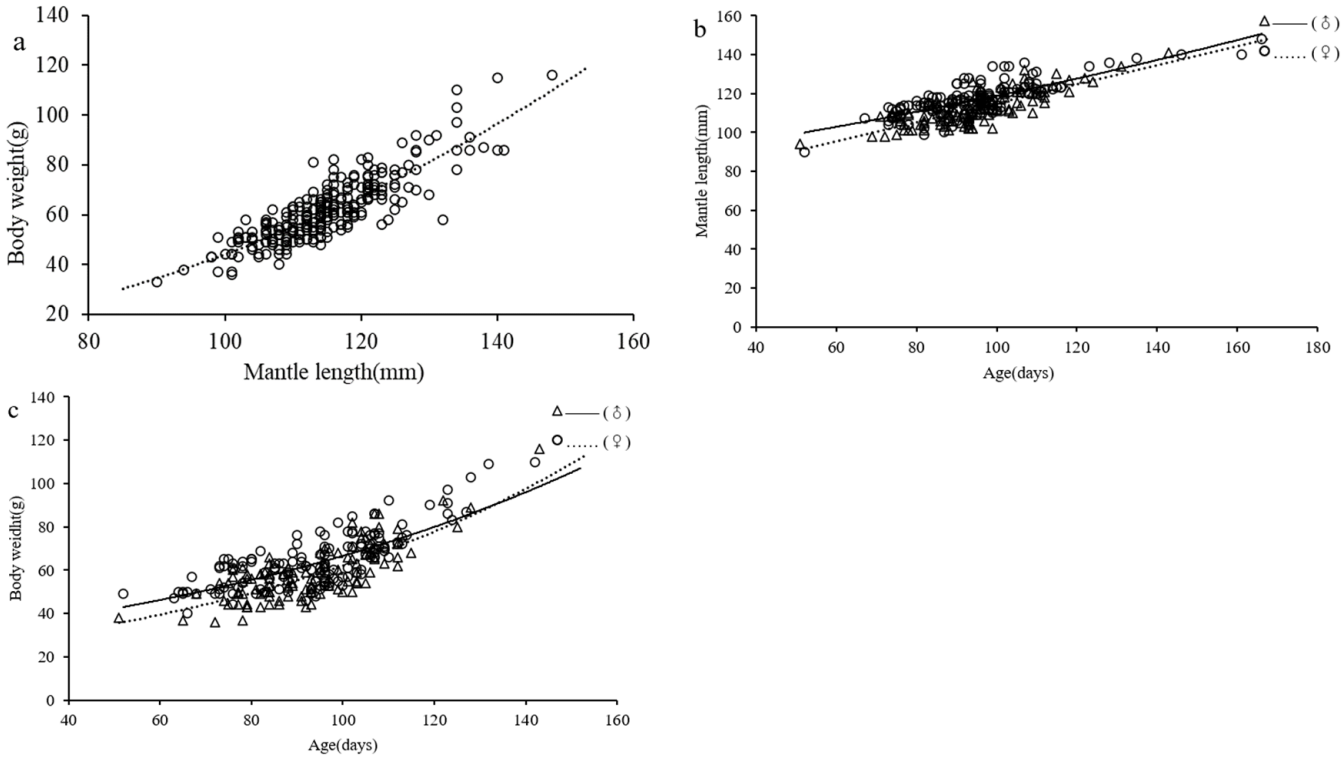

Figure 7. ML–BW (**a**), ML–age (**b**), and BW–age (**c**) relationships of *B. magister shevtsovi*.

BW–ML growth model:

$$W = 0.001\ L^{2.3273}\ (R^2 = 0.7420,\ n = 261)$$

ML–age growth model for females:

$$ML = 0.4328\ Age + 75.893\ (R^2 = 0.5939,\ n = 150)$$

ML–age growth model for males:

$$ML = 74.092\ e^{0.0044Age}\ (R^2 = 0.6155,\ n = 111)$$

BW–age growth model for females:

$$BW = 26.769\ e^{0.0091Age}\ (R^2 = 0.6088,\ n = 150)$$

BW–age growth model for males:

$$BW = 20.046\ e^{0.0113Age}\ (R^2 = 0.6397,\ n = 111)$$

3.6. Growth Rate

The ANCOVA indicated that both the average of IGRs for ML ($p = 0.020 < 0.05$) and BW ($p = 0.023 < 0.05$) and the AGRs for ML ($p = 0.031 < 0.05$) and BW ($p = 0.046 < 0.05$) differed significantly between sexes. With the increase of age, the AGRs and IGRs of ML and BW of females were higher than males. The average AGRs and IGRs for ML were 1.787 mm/d and 1.790 for females and 1.764 mm/d and 1.328 for males, respectively, and the average AGRs and IGRs for BW were 3.12 g/d and 4.209 for females and 2.656 g/d and 2.876 for males, respectively (Table 2).

Table 2. Instantaneous relative growth rates (IGRs) and absolute growth rate (AGR) for mantle length (ML) and body weight (BW) of the autumn group of *B. magister shevtsovi* in the Japan Sea.

	Age-Class (d)	Sample Number	Mantle Length			Body Weight		
			Average of ML (mm)	IGR	AGR (mm^{-1})	Average of BW (g)	IGR	AGR (g^{-1})
females	41–60	2	120.00	0.18	0.21	67.50	0.70	1.27
	61–80	34	115.15	1.44	1.68	62.06	4.98	3.32
	81–100	52	116.77	1.86	2.22	63.34	4.04	3.21
	101–120	42	117.38	2.39	2.84	64.97	5.87	4.11
	121–140	15	120.93	1.74	2.13	62.27	4.84	3.88
	141–160	3	111.67	1.92	2.10	63.67	3.02	2.40
	161–180	2	113.00	1.18	1.33	65.00	6.01	3.67
males	41–60	2	110.00	1.09	1.20	59.00	0.47	2.44
	61–80	29	109.24	2.15	2.31	54.17	3.32	2.94
	81–100	43	110.84	1.56	1.79	56.14	2.61	2.79
	101–120	26	114.00	1.70	2.05	61.62	4.10	2.11
	121–140	10	119.10	1.23	1.47	71.10	3.88	3.00
	141–160	1	121.00	/	/	75.00	/	/

The maximum AGR (Figure 8a) and IGR (Figure 8b) values for ML were 2.84 mm/d and 2.389%/d for the females, within 101–120 days, and the maximum AGR (Figure 8a) and IGR (Figure 8b) values were 2.32 mm/d and 2.15%/d for males within 61–80 days.

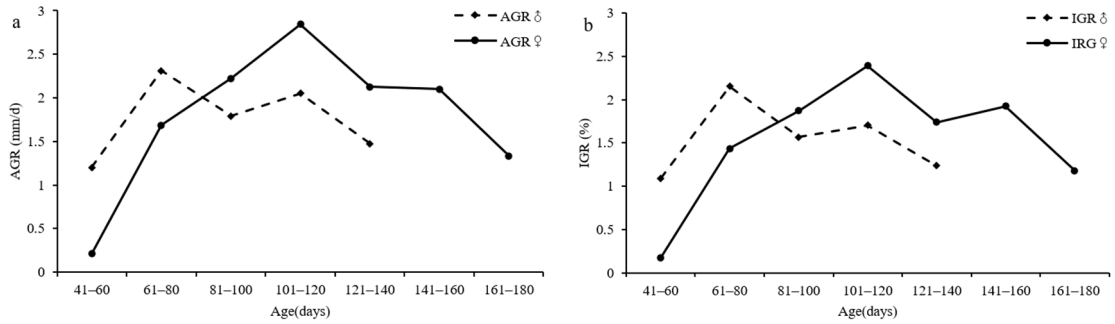

Figure 8. Relationships between the ML growth rate and age of *B. magister shevtsovi* samples: (**a**) AGR; (**b**) IGR.

The maximum AGR (Figure 9a) and IGR (Figure 9b) values for BW were 4.11 g/d and 5.87%/d for the females, respectively, within 101–120 days. For the male samples, the AGR peaked value of 2.94 g/d within 61–80 days; the lowest value was 2.105 g/d within 101–120 days (Figure 9a). The IGR trend gradually increased and then decreased, and the IGR value peaked at 3.32%/d (Figure 9b, Table 2).

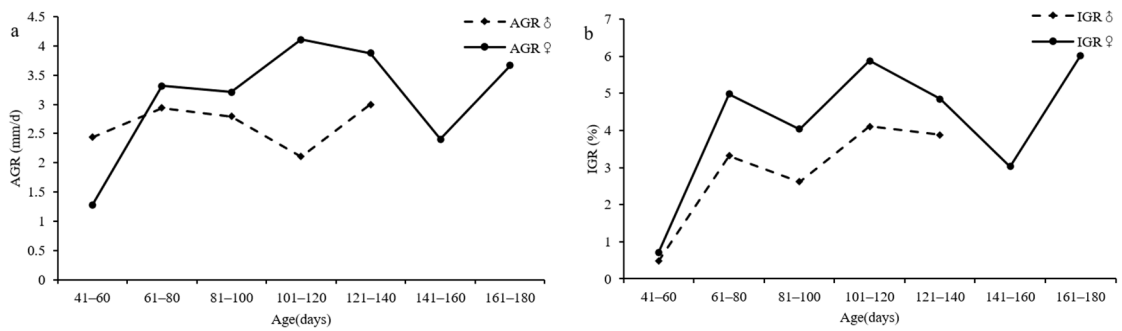

Figure 9. Relationships between the BW growth rate and age of *B. magister shevtsovi* samples: (**a**) AGR; (**b**) IGR.

4. Discussion

4.1. Morphological Characteristics

B. magister shevtsovi lives in the sea with high latitude and low sea surface temperatures [1]. Compared with the external morphology of squid belonging to the same genus, the ML of *B. magister shevtsovi* was stout and cylindrical, with a smaller body size and larger fins, which may be caused by the different hydrological environments [1,32]. The ML of *B. magister shevtsovi* was generally less than 200 mm [4], and the maximum ML in this study was 148 mm, which was consistent with the above conclusion. The rhomboid fin of *B. magister shevtsovi* was approximately 50% of the ML, which might be related to the complex ocean currents in the Japan Sea. Under the action of the Japanese warm current and Kuril cold current, the cold and warm currents converged to form a flow barrier, which brought abundant baits [33]. The developed fins of *B. magister shevtsovi* can increase its swimming speed [34], thus improving its hunting efficiency.

The results of this study showed that the proportion of males was larger when ML < 110 mm, while the proportion of females increased rapidly when ML > 110 mm. The BW distribution was similar to ML. When BW < 50 g, the proportion of males was larger, while when BW > 50 g, the proportion of females increased rapidly. This may be related to the different stages of growth and development of *B. magister shevtsovi*. The reproduction of the *B. magister shevtsovi* is carried out in deep water. As the juvenile stage gradually grow into the subadult stage, the living layer of the *B. magister shevtsovi* transitions to the middle and upper layer [16], which may be the reason for the different percentage of ML and BW of females and males in different periods. In addition, studies have shown that the female body size of the *B. magister shevtsovi* of the Japan Sea is smaller than northwest Pacific and have lower fecundity but higher survival rates [1,35], which may be related to the specific marine conditions in the Japan Sea.

4.2. Statolith Microstructure

In this study, it was found that in the statolith of *B. magister shevtsovi* from the NZ to PZ, the brightness of the rings changed from dark to light and then to dark, and the distance between the rings changed from narrow to wide and then to the narrowest. The transition zone between P and DZ was the darkest, and the width of the growth rings changed from narrow to wide, which was easy to count, while PZ was the opposite, which was difficult to count. This is consistent with other methods to read the age of squid statolith from NZ to P, then to DZ, and finally to PZ [12].

According to the analysis, the growth characteristics of each zone in the microstructure of the statolith are closely related to the development of the individual [19]. The P is formed in the larval stage, the DZ in the juvenile stage, and the PZ in the subadult and adult stages [36,37]. The microstructures of the statolith of *B. magister shevtsovi* showed that the larvae were in the endogenous nutrition stage and did not start predation, so the growth was relatively slow, and the distance between the rings in the P was narrow. In the juvenile stage, individuals are in the stage of exogenous nutrition, taking in food from the outside and growing faster, so the distance between the ringlets in the DZ was wider [37,38]. Combined with the development characteristics of *B. magister shevts'vi's* life history and the changes in the microstructure of statolith, it can be fully proven that it was scientific and effective to judge the growth characteristics of statolith by using the microstructure. In addition, some scholars believe that the ordering pattern of squid statolith rings is related to individual growth [37], sex maturity [2], habitat, and food [39]. The energy obtained in the juvenile stage is mainly used for its growth and development, while the energy obtained in the subadult and adult stages is mainly used for sex maturity [1]. In the adult stage, the individual growth was basically stable, which explained the slow growth of the PZ of the statolith microstructure of *B. magister shevtsovi*.

Other studies have shown that the arrangement of the DZ and PZ of the statolith microstructure of cephalopods was related to feeding habits [37] and vertical movement [27]. With the development of *B. magister shevtsovi*, the intensity of feeding changed, which

affected the microstructure of the statolith to a certain extent [2]. The subday increments are incomplete rings in the middle of the dark band of the day increments, which has no obvious ring [40]. This study also found that there were many subday increment rings during the transition from P to DZ, which were also found in the studies of *Dosidicus gigas* [41]. The appearance of the subday increments had a certain degree of influence on the counting of the rings, so in the counting of growth rings, we must pay attention to the distinction between the sun and the subday increments.

4.3. Age Structure and Maturity

The age and growth patterns of several cephalopods reported in previous studies can be reliably assessed by the daily increments on the beak by comparing statolith increments observed under artificial feeding conditions [24,42]. The age ranged from 52 to 166 days and 51 to 143 days, both with a high concentration in 61–140 d, accounting for 95.34 and 97.30 percent for females and males, respectively (Figure 5). The longevity of the samples in this study was similar to the squid from the ETPO equatorial waters [43] and the Bay of Bengal [44], where the estimated longevity of this squid was no more than 6 months. The *B. magister shevtsovi* age was mainly 60–120 days (3–4 months). It was confirmed that males more quickly reached the mature stage than females at the same age stage [45], and this phenomenon was also commonly found in other Ommastrephidae species [46,47]. The longevity of squid shows geographic variation, and many factors affect this phenomenon, such as temperature and food availability [48]. Generally, squid living in cold waters with lower temperatures and higher food availability have a longer life span than those living in tropical waters [48]. However, in this study, the life span of *B. magister shevtsovi* was relatively short, and we speculate that the age composition of *B. magister shevtsovi* may be related to its own growth characteristics. *B. magister shevtsovi* has a life span of one year and dies after spawning, which was also found in a previous study, similar to a common phenomenon in squid growth [4].

In this study, the majority of sexual maturity of *B. magister shevtsovi* was most in stages I and II, a small number of samples were in stages III and IV. With the increase of sexual maturity, the proportion of male and female *B. magister shevtsovi* samples decreased gradually, and no individual was found in stages V, which may be related to the reproductive characteristics of the *B. magister shevtsovi* that die after spawning [1]. In this study, the proportion of males which were in stages I–IV was larger than females, this phenomenon confirmed that male *B. magister shevtsovi* had earlier sexual maturation than females [16]. In addition, males of the northwestern Indian Ocean *Sthenoteuthis oualaniensis* reached the mature stage faster than females too [49], which may be due to the marine environmental conditions and its own growth characteristics. In general, most of the *B. magister shevtsovi* samples collected this time did not reach sexual maturity. In the future study, we will extend the sampling time and increase the number of samples, to provide reference for the scientific analysis and protection of *B. magister shevtsovi* resources.

4.4. Hatching Date and Population Structure

According to the statolith age, the hatching population *B. magister shevtsovi* could be calculated by combining with the catch date. The hatching peak of the squid was mainly in July, August, and September, so we speculated that they belonged to the autumn group. The squid has a short life span of only one year and dies after spawning [4]. In addition, the hydrology of the squid is special, and its vertical distribution in the Japan Sea is not uniform. Its distribution depth varies from 50–120 m to 300–500 m in different periods [1]. At present, there are few studies on the spawning and early life history of *B. magister shevtsovi*, and the hatching group division is not clear, which is largely related to the uniqueness of growth and development [36]. Due to the influence of geographical isolation, different subspecies diverge. Some studies have shown that there are significant differences between the populations of *B. magister shevtsovi* in the Northwest Pacific Ocean and in the Japan Sea [1]. The results of a study on squid from the Northwest Pacific Ocean

showed that the spawning period was long, with at least two peak spawning periods in summer, autumn, and winter [3,50]. The growth and reproduction of cephalopods are related to their own growth characteristics [21], appropriate temperature, and habitat water layer [2]. The most notable feature of *B. magister shevtsovi* in the Japan Sea is that the temperature of the habitat area is low, ranging from 0.2–1.5 °C, which may have a certain impact on population growth. In this study, only the autumn group was found in the study of *B. magister shevtsovi* in the Japan Sea. The population division of *B. magister shevtsovi* was initially discussed through a single annual sampling, and the sampling time and sample size will be extended in a subsequent study.

4.5. Growth Models

In the relationship between ML and BW, conditional factor a and allometric growth factor b were important parameters in the assessment of fishery resources [51]. Factor a can represent the environmental conditions of population growth, which change with changes in food, hydrology, and other environmental factors in the habitat [52]. The results of this study showed that a was higher in the relationship between ML and BW (a = 0.001), which indicated that the marine environment in the catch area had better hydrological conditions and was suitable for the growth of *B. magister shevtsovi*. B < 3 (b = 2.3273) indicated negative allometric growth in this population, namely, the growth rate of ML was faster than that of BW [53]. This may be due to the complex and varied seabed topography in this area, which provided abundant nutrients and natural shelter [54] and promoted the growth of *B. magister shevtsovi*.

We described the ML–age and BW–age relationships separately of males and females because significant differences were found between the sexes. The best growth models for the ML–age of females and males were expressed by linear and exponential, respectively. The best growth models for the BW–age of females and males were both expressed by exponential models. At present, there is a lack of studies on the growth model of the *B. magister shevtsovi*. Compared with other cephalopods, the growth model of the *B. magister shevtsovi* was partially similar. For example, linear growth model was the best fit for ML–age relationships of the autumn population of *S. oualaniensis* in the Northwest Indian Ocean [49]. Exponential growth model was the best fit for the ML–age relationships of *S. oualaniensis* in the South China Sea [55]. Power and linear growth models best described the ML–age relationship of winter population of *Illex argentinus*, while exponential and logarithmic growth models were the best fit for the ML–age relationship in an autumn population [12]. The age and growth of squid are both affected by many factors, and optimal growth equations may differ among different squid sexes, populations, and different growth stages [27]. With the growth of the *B. magister shevtsovi*, its habitat water layer changed [1], which may be an important factor affecting its growth.

4.6. Growth Rate

The average AGRs and IGRs for ML were 1.787 mm/d and 1.790 for females and 1.764 mm/d and 1.328 for males, respectively, and the average AGRs and IGRs for BW were 3.12 g/d and 4.209 for females and 2.656 g/d and 2.876 for males, respectively. The maximum AGRs and IGRs for ML were 2.84 mm/d and 2.39 for females and 2.32 mm/d and 2.15 for males, and the maximum AGRs and IGRs for BW were 4.11 g/d and 5.87 for females and 2.32 g/d and 2.15 for males in this study. With increasing age, the AGR of individual males and females of *B. magister shevtsovi* showed similar patterns, with two similar peaks. The ML of females increased rapidly from 41–120 days and gradually decreased after 120 days, while the ML of males peaked at 60–80 days and then decreased gradually. The AGR for BW of males and females of *B. magister shevtsovi* also showed similar peaks at 61–100 d and 100–140 d, respectively. Therefore, we speculated that the AGR for ML and BW continued to increase before *B. magister shevtsovi* reached first maturity. The results of this study showed that the male sexual maturation stage was earlier than that of the female, which was also found in other cephalopods [56]. Males reached the first sexual

maturation at 80–100 days (3 months), and females reached the first sexual maturation at 120–140 days (4 months). The results of this study are similar to those of other cephalopods at the age of reaching primary sexual maturity (3–5 months), such as *I. argentinus* [24], *Illex coindetii* [57,58], and *D. gigas* [46,59]. This may be because before reaching sexual maturity, the energy intake of the *B. magister shevtsovi* is mostly used for individual growth, and when the individual reaches a certain length, more energy is used for gonadal development [2]. In addition, the age and growth of cephalopods are affected and acted upon by many factors. The size, food source, and environmental factors of the squid have obvious effects on their growth style and life span [60]. It has been shown that lower temperatures reduce growth rates and delay maturation of squid and that higher temperatures promote growth rates and maturation in warmer low–latitude waters [48]. However, *B. magister shevtsovi* is distributed in cold and high latitude waters, and the specific effects of the environment on its growth and development need to be further studied.

5. Conclusions

In this study, we studied the growth, age composition, and population division of *B. magister shevtsovi* based on statolith microstructure, which proved the feasibility of using statolith microstructure to determine age. The results showed that most of the samples of *B. magister shevtsovi* were autumn populations. The period from 80–120 days (3–4 months) was considered to correspond to the subadult stage in the whole life history of *B. magister shevtsovi* in the Japan Sea. Research on the growth and age of *B. magister shevtsovi* is still lacking, and the optimal growth model may be different in different environments. In addition, the existence of other populations of *B. magister shevtsovi* needs to be further explored. Therefore, to study the growth and population division of *B. magister shevtsovi*, in future, we will extend the sampling time, expand the sampling area, and increase the sampling volume to provide a scientific basis for the exploitation and utilization of *B. magister shevtsovi* resources.

Author Contributions: Conceptualization, H.L. and X.C.; methodology, H.L.; software, Y.O.; validation, H.L., Y.O. and Y.T.; formal analysis, Y.O.; investigation, Y.T.; resources, H.L.; data curation, H.L.; writing—original draft preparation, Y.O.; visualization, Z.C.; supervision, Z.C.; project administration, H.L.; funding acquisition, H.L. All authors have read and agreed to the published version of the manuscript.

Funding: This research was funded by the Natural Science Foundation of China (NSFC 41506184) and National Key Research and Development Program of China 489 (2019YFD0901402).

Institutional Review Board Statement: The study was conducted according to the guidelines of the Code of Ethics of the University Department of Marine Studies (No. nhdf2022-07); we only used specimens obtained from the surveys that were already dead.

Informed Consent Statement: Not applicable.

Data Availability Statement: The datasets used and/or analyzed during the current study available from the corresponding author on reasonable request.

Acknowledgments: We would like to express our thanks to support for two scientific surveys made by "*Zhouyu 678*" is gratefully acknowledged. Thanks for the partial support of the Natural Science Foundation of China (NSFC 41506184) and National Key Research and Development Program of China 489 (2019YFD0901402). Finally, we thank the editor and the anonymous reviewers whose comments greatly improved the manuscript.

Conflicts of Interest: The authors declare no conflict of interest.

References

1. Katugin, O.N. A new subspecies of the schoolmaster gonate squid, *Berryteuthis magister* (Cephalopoda: Gonatidae), from the Japan Sea. *Veliger* **2000**, *43*, 82–97.
2. Wang, H.H.; He, T.; Lu, H.J.; Chen, Z.Y.; Ning, X.; Chen, X.J. Fisheries biology characteristics of *Berryteuthis magister* shevtsovi in the Japan Sea. *Chin. J. Ecol.* **2021**, *40*, 2467–2477.

3. Nesis, K.N. Population dynamics of the *Berryteuthis magister* Commander (Berry) in the Western Bering Sea during the autumn spawning season. *Ruthenica* **1995**, *5*, 55–69.
4. Chen, X.J.; Liu, B.L.; Wang, Y.G. *Cephalopods in the World*; China Ocean Press: Beijing, China, 2009; pp. 273–306.
5. Chen, X.Y.; Lu, H.J.; He, J.R.; Wang, H.H.; Liu, K.; Chen, Z.Y.; Chen, X.J. Analysis of Beak Morphological Characteristic of *Berryteuthis magister shevtsovi* in Japan Sea. *Chin. J. Zool.* **2021**, *56*, 918–928.
6. Zhu, W.B.; Chen, X.Y.; Lu, H.J.; Chen, Z.Y.; Ning, X.; Cui, G.C.; Guo, A.; Chen, X.J. Analysis of pigmentation characteristics on beak of *Berryteuthis magister shevtsovi* in the Japan Sea based on artificial neural networks. *J. Fish. China* **2022**, *46*, 950–958.
7. Trotsenko, B.G.; Pinchukov, M.A. Mesoscale distribution features of the purpleblack squid *Sthenoteuthis oualaniensis* with reference to the structure of the upper quasi-homogeneous layer in the West India Ocean. *Oceanology* **1994**, *34*, 380–385.
8. Perales, R.C.; Almansa, E.; Aurora, B.; Beatriz, C.F.; José, I.; Francisco, J.S.; José, F.C.; Carmen, R. Age Validation in Octopus vulgaris Beaks Across the Full Ontogenetic Range: Beaks as Recorders of Life Events in Octopuses. *J Shellfish. Res.* **2014**, *33*, 481–493. [CrossRef]
9. Radtke, R.L. Chemical and structural characteristics of statoliths from the short-finned squid *Illex illecebrosus*. *Mar. Biol.* **1983**, *76*, 47–54. [CrossRef]
10. Bettencourt, V.; Guerra, A. Growth increments and biomineralization process in cephalopod statoliths. *J. Exp. Mar. Biol. Ecol.* **2000**, *248*, 191–205. [CrossRef]
11. Semmens, J.; Moltschaniwskyj, N. An examination of variable growth in the loliginid squid *Sepioteuthis lessoniana*: A whole animal and reductionist approach. *Mar. Ecol. Prog. Ser.* **2000**, *193*, 135–141. [CrossRef]
12. Lu, H.J.; Chen, X.J.; Fang, Z. Comparison of the beak morphologic growth characteristics between two spawning populations of *Illex argentinus* in Southwest Atlantic Ocean. *J. Ocean Univ. China* **2012**, *42*, 33–40.
13. Agus, B.; Carugati, L.; Bellodi, A.; Cannas, R.; Cau, A.; Cera, J.; Coluccia, E.; Melis, R.; Ruiu, S.; Cuccu, D. Molecular and Biological Analysis on *Ommastrephes caroli* Findings in the Central Western Mediterranean Sea (Sardinian Waters) Including First Age Investigation Using Eye Lenses and Beaks. *Front. Mar. Sci.* **2021**, *8*, 683856. [CrossRef]
14. Arkhipkin, A.I.; Shcherbich, Z.N. Thirty years' progress in age determination of squid using statoliths. *J. Mar. Biol. Assoc. UK* **2012**, *92*, 1389–1398. [CrossRef]
15. Lu, H.J.; Wang, C.J.; Chen, X.J. Preliminary study on the biological characteristics of *Sthenoteuthis oualaniensis* in the high seas nearby the equator of eastern Pacific during April to June. *J. Shanghai Ocean Univ.* **2014**, *23*, 441–447.
16. Dong, Z.Z. *Cephalopod Biology of the World's Oceanic Economy*; Shandong Science and Technology Press: Jinan, China, 1991; pp. 27–105.
17. Fang, Z.; Xu, L.; Chen, X.; Liu, B.; Li, J.; Chen, Y. Beak growth pattern of purpleback flying squid *Sthenoteuthis oualaniensis* in the eastern tropical Pacific equatorial waters. *Fish. Sci.* **2015**, *81*, 443–452. [CrossRef]
18. Arkhipkin, A.I. Reproductive System Structure, Development and Function in Cephalopods with a New General Scale for Maturity Stages. *J. Northwest Atl. Fish. Sci.* **1985**, *12*, 63–74. [CrossRef]
19. Chen, X.; Lu, H.; Liu, B.; Chen, Y. Age, growth and population structure of jumbo flying squid, *Dosidicus gigas*, based on statolith microstructure off the Exclusive Economic Zone of Chilean waters. *J. Mar. Biol. Assoc. UK* **2010**, *91*, 229–235. [CrossRef]
20. Lu, H.-J.; Chen, X.-J. Age, growth and population structure of *Illex argentinus* based on statolith microstructure in Southwest Atlantic Ocean. *J. Fish. China* **2012**, *36*, 1049–1056. [CrossRef]
21. Lu, H.J.; Zhang, X.; Tong, Y.H.; Tang, Y.; Liu, K.; Liu, W.; Chen, X.J. Statolith microstructure and growth characteristics of *Sthenoeuthis oualaniensis* in the Xisha Islands waters of the South China Sea. *J. Fish. China* **2020**, *44*, 767–776.
22. Yatsu, A.; Midorikawa, S.; Shimada, T.; Uozumi, Y. Age and growth of the neon flying squid, *Ommastrephes bartrami*, in the North Pacific ocean. *Fish. Res.* **1997**, *29*, 257–270. [CrossRef]
23. Liu, B.L.; Chen, X.J.; Chen, Y.; Hu, G.Y. Determination of squid age using upper beak rostrum sections: Technique improvement and comparison with the statolith. *Mar. Biol.* **2015**, *162*, 1685–1693. [CrossRef]
24. Rodhouse, P.G.; Hatfield, E.M.C. Dynamics of Growth and Maturation in the Cephalopod *Illex argentinus* de Castellanos, 1960 (Teuthoidea: Ommastrephidae). *Philos. Trans. R. Soc. Lond. B Biol. Sci.* **1990**, *329*, 229–241.
25. Froese, R.; Thorson, J.T.; Reyes, R.B. A Bayesian approach for estimating length-weight relationships in fishes. *J. Appl. Ichthyol.* **2013**, *30*, 78–85. [CrossRef]
26. Jackson, G.D. Application and Future Potential of Statolith Increment Analysis in Squids and Sepioids. *Can. J. Fish. Aquat. Sci.* **1994**, *51*, 2612–2625. [CrossRef]
27. Arkhipkin, A.I. Age and growth of the mesopelagic squid *Ancistrocheirus lesueurii* (Oegopsida: *Ancistrocheiridae*) from the central-east Atlantic based on statolith microstructure. *Mar. Biol.* **1997**, *129*, 103–111. [CrossRef]
28. Malcolm, H. *Modeling and Quantitative Methods in Fisheries*; Chapman and Hall/CRC: New York, NY, USA, 2001; pp. 227–232.
29. Hiramatsu, K. Application of Maximum Likelihood Method and AIC to Fish Population Dynamics. In *Fish Population Dynamics and Statistical Models*; Matsumiya, Y., Ed.; Koseisha Koseikaku: Tokyo, Japan, 1993; pp. 9–21.
30. Imai, C.; Sakai, H.; Katsura, K.; Honto, W.; Hida, Y. Growth model for the endangered cyprinid fish *Tribolodon nakamurai* based on otolith analyses. *Fish. Sci.* **2002**, *68*, 843–848. [CrossRef]
31. Arkhipkin, A.I.; Roa-Ureta, R. Identification of ontogenetic growth models for squid. *Mar. Freshw. Res.* **2005**, *56*, 371–386. [CrossRef]

32. Okutani, T.; Tagawa, M.; Horikawa, H. *Cephalopods from Continental Shelf and Slope around Japan*; Japan Fisheries Resource Conservation Society: Tokyo, Japan, 1988.
33. Tang, F.H.; Shi, Y.R.; Zhu, J.X.; Wu, Z.L.; Wu, Y.M.; Cui, X. Influence of marine environment factors on temporal and spatial distribution of Japanese common squid fishing grounds in the Japan Sea. *J. Fish. China* **2015**, *22*, 1036–1043.
34. Zhou, Y.Q. Study on the maximum swimming speed of fishes. *J. Fish. China* **1985**, *9*, 105–120.
35. Alexander, I.A.; Vyacheslav, A.B.; Andrey, V.V. Distribution and growth in juveniles of the squid *Berryteuthis magister* (Cephalopoda, Gonatidae) in the western Bering Sea. *Sarsia* **1998**, *83*, 45–54.
36. Arkhipkin, A.I. Statoliths as 'black boxes' (life recorders) in squid. *Mar. Freshw. Res.* **2005**, *56*, 573–583. [CrossRef]
37. Wang, H.H.; Lu, H.J.; He, J.R.; Liu, K.; Chen, X.Y.; Chen, X.J. Microstructures and growth characteristics of statoliths from *Sthenoeuthis oualaniensis* in the northwest Indian Ocean. *Chin. J. Appl. Ecol.* **2022**, 1–9. [CrossRef]
38. Chen, X.J.; Liu, B.L. *Fishery Resources Biology*; Science Press: Beijing, China, 2017; pp. 58–62.
39. Ma, J.; Chen, X.J.; Liu, B.L.; Lu, H.J.; Li, S.L.; Cao, J. Review of the influence of environment factors on microstructure of statoliths of cephalopod. *J. Shanghai Ocean Univ.* **2009**, *5*, 616–622.
40. Hu, G.Y.; Chen, X.J.; Liu, B.L.; Fang, Z. Microstructure of statolith and beak for *Dosidicus gigas* and its determination of growth increments. *J. Fish. China* **2015**, *39*, 361–370.
41. Wang, Y.P.; Chen, X.J.; Fang, Z.; Li, J.H.; Li, Z.Q.; Chen, L.F. Statolith Morphology of Jumbo Flying Squid (*Dosidicus gigas*) in Waters Near the Equator of Eastern Pacific Ocean. *J. Oceanol. Limnol.* **2019**, 147–156. [CrossRef]
42. Hu, G.; Fang, Z.; Liu, B.; Yang, D.; Chen, X.; Chen, Y. Age, growth and population structure of jumbo flying squid *Dosidicus gigas* off the Peruvian Exclusive Economic Zone based on beak microstructure. *Fish. Sci.* **2016**, *82*, 597–604. [CrossRef]
43. Liu, B.L.; Chen, X.J.; Li, J.H.; Chen, Y. Age, growth and maturation of *Sthenoteuthis oualaniensis* in the eastern tropical Pacific Ocean by statolith analysis. *Mar. Freshw. Res.* **2016**, *67*, 1973–1981. [CrossRef]
44. Sukramongkol, N.; Promjinda, S.; Prommas, R. Age and Reproduction of Sthenoteuthis Oualaniensis in the Bay of Bengal. In Proceedings of the Ecosystem-Based Fishery Management in the Bay of Bengal, Phuket, Thailand, 14 December 2007; Department of Fisheries (DOF), Ministry of Agriculture and Cooperatives: Bangkok, Thailand, 2007; pp. 195–205.
45. Chen, Z.Y.; Lu, H.J.; Liu, W.; Liu, K.; Chen, X.J. Beak Microstructure Estimates of the Age, Growth, and Population Structure of Purpleback Flying Squid (*Sthenoteuthis oualaniensis*) in the Xisha Islands Waters of the South China Sea. *Fishes* **2022**, *7*, 187. [CrossRef]
46. Markaida, U.; Quiñonez-Velázquez, C.; Sosa-Nishizaki, O. Age, growth and maturation of jumbo squid *Dosidicus gigas* (Cephalopoda: Ommastrephidae) from the Gulf of California, Mexico. *Fish. Res.* **2004**, *66*, 31–47. [CrossRef]
47. Watanabe, H.; Kubodera, T.; Ichii, T.; Sakai, M.; Moku, M.; Seitou, M. Diet and sexual maturation of the neon flying squid *Ommastrephes bartramii* during autumn and spring in the Kuroshio–Oyashio transition region. *J. Mar. Biol. Assoc. UK* **2008**, *88*, 381–389. [CrossRef]
48. Arkhipkin, A.I.; Steven, E.C.; Jennifer, F.G.; Simon, R.T. Spatial and temporal variation in elemental signatures of statoliths from the Patagonian longfin squid (*Loligo gahi*). *Can. J. Fish. Aquat.* **2004**, *61*, 1212–1224. [CrossRef]
49. Lu, H.-J.; Ou, Y.-Z.; He, J.-R.; Zhao, M.-L.; Chen, Z.-Y.; Chen, X.-J. Age, Growth and Population Structure Analyses of the Purpleback Flying Squid *Sthenoteuthis oualaniensis* in the Northwest Indian Ocean by Beak Microstructure. *J. Mar. Sci. Eng.* **2022**, *10*, 1094. [CrossRef]
50. Fedorets, Y.A. Seasonal Distribution of the Squid *Berryteuthis magister* in the Western Bering Sea. In *Systematics and Ecology of Cephalopods*; Zoological Institute of Academy of Sciences of the USSR: Leningrad, Russia, 1983; pp. 129–130.
51. Fei, H.N.; Zhang, S.Q. *Aquatic Resources*; China Science and Technology Press: Beijing, China, 1990; pp. 245–254.
52. Froese, R. Cube law, condition factor and weight–length relationships: History, meta-analysis and recommendations. *J. Appl. Ichthyol.* **2010**, *22*, 241–253. [CrossRef]
53. Seiyaboh, E.I.; Harry, G.A.; Izah, S.C. Length-Weight Relationship and Condition Factor of Five Fish Species from River Brass, Niger Delta. *Int. J. Agric. Biol.* **2016**, *4*, 37–44.
54. Hu, X.M.; Xiong, X.J.; Qiao, F.L.; Guo, X.P. Surface current field and seasonal variability in the *Kuroshio andadjacent* regions derived from satellite-tracked drifter data. *Acta Oceanol. Sin.* **2008**, *30*, 11–29.
55. Zhao, C.X.; Chen, Z.P.; He, X.B.; Deng, Y.S.; Feng, B.; Yan, Y.R. Age, growth and population structure of purple beak flying squid, *Sthenoteuthis oualaniensis* the south China Sea in spring based on statolith microstructure. *Acta Hydrobiol. Sin.* **2017**, *41*, 884–890.
56. Jereb, P.; Roper, C.F.E. Cephalopods of the World. In *An Annotated and Illustrated Catalog of Cephalopod Species Known to Date*; Volume 2: Myopsid and Oegopsid Squids; FAO: Rome, Italy, 2010; pp. 315–318.
57. Arkhipkin, A.; Jereb, P.; Ragonese, S. Growth and maturation in two successive seasonal groups of the short-finned squid, *Illex coindetii* from the Strait of Sicily (central Mediterranean). *ICES J. Mar. Sci.* **2000**, *57*, 31–41. [CrossRef]
58. Petrić, M.; Škeljo, F.; Šifner, S.K. Age, growth and maturation of *Illex coindetii* (Cephalopoda: Ommastrephidae) in the eastern Adriatic Sea. *Reg. Stud. Mar. Sci.* **2021**, *47*, 101935. [CrossRef]
59. Mejía-Rebollo, A.; Quiñónez-Velázquez, C.; Salinas-Zavala, C.A.; Salinas, Z.; Markaida, U. Age, growth and maturity of jumbo squid (*Dosidicus gigas* d'orbigny, 1835) off the Western Coast of the baja California peninsula. *Cal. Coop. Ocean. Fish.* **2008**, *49*, 256–262.
60. Arkhipkin, A.I. Towards identification of the ecological lifestyle in nektonic squid using statolith morphometry. *J. Molluscan Stud.* **2003**, *69*, 171–178. [CrossRef]